Supporting information

Structure design of BiOF solid electrolyte with remarkably outstanding fluoride-ion diffusion performance induced by Ga doping

Jiyu Ning,‡[a] Weijia Meng,‡[a] Chuang Wang,[a] Huangkai Wang,[a] Chao Wu,[a] Lidong You,[a] Xianyou Wang,[b] Yong Pei,[b] Haibo Wang,[c] Zhenhua Yang[a,*]

[a]Key Laboratory of Low Dimensional Materials & Application Technology of Ministry of Education, School of Materials Science and Engineering, Xiangtan University, Xiangtan 411105, Hunan, China

[b]Key Laboratory of Environmentally Friendly Chemistry and Applications of Ministry of Education, Hunan Province Key Laboratory of Electrochemical Energy Storage and Conversion, School of Chemistry, Xiangtan University, Xiangtan 411105, Hunan, China.

[c]NanChang JiaoTong Institute, Nanchang 330100, Jiangxi, China

---

*[*]Corresponding authors. Address: *Key Laboratory of Low Dimensional Materials & Application Technology of Ministry of Education, School of Materials Science and Engineering, Xiangtan University, Xiangtan 411105, Hunan, China*.

E-mail address: yangzhenhua@xtu.edu.cn (Zhenhua Yang)

[†]Electronic supplementary information(ESI) available.

[‡]These authors contributed equally to this work.

1. Crystal structure and band structure of BiOF
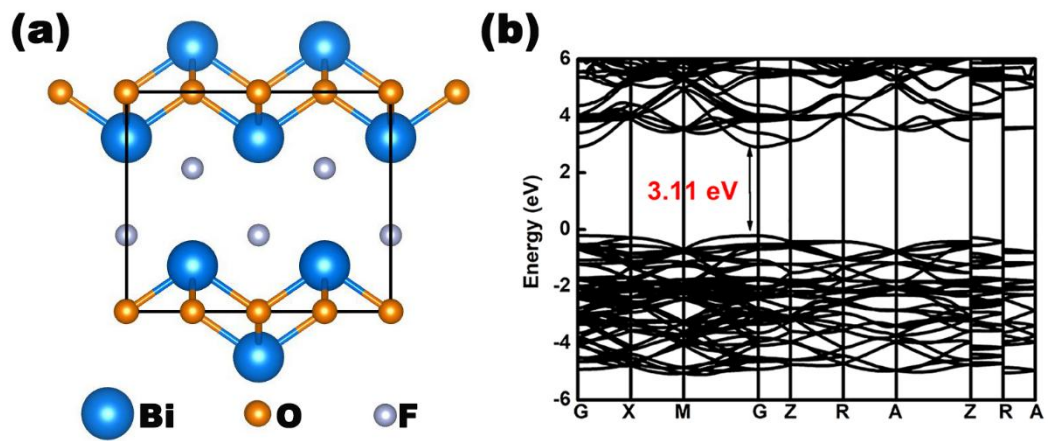

Fig. S1 (a) Crystal structure (front view) and (b) band structure of BiOF.

2. Investigation of formation energies

**Table S1.**Space group and calculated formation enthalpies of phases in the Bi-O-F system

Compounds	Space group	Formation enthalpies (eV)	Ref(eV)
BiO_2	$Fm\bar{3}m$	-3.87	-3.49[1]
Bi_2O_3	$P1$	-7.37	-6.48[2]
Bi_2O_5	$Pbam$	-7.22	-7.58[1]
Bi_3O_5	$C12/c1$	-11.74	
Bi_3O_7	$Pnma$	-11.00	
Bi_4O_5	$C1c1$	-11.85	
Bi_4O_7	$P1$	-16.55	
Bi_4O_9	$P4/n1$	-13.74	
BiF_3	$Pnma$	-8.80	-8.69[3]
BiF_4	$I4/mmm$	-9.93	
BiF_5	$I4/m$	-10.69	

Table S2. Space group and calculated formation enthalpies of Ga-O and Ga-F compounds

Compounds	Space group	Formation enthalpies(eV)	Ref(eV)
GaO	$P6_3mc$	-2.41	
GaO$_2$	$Pnma$	-4.52	
GaO$_3$	$Im\overline{3}$	-2.05	
Ga$_2$O$_3$	$R\overline{3}c$	-10.81	-10.73[4]
Ga$_3$O$_5$	$Pnma$	-15.29	
GaF$_3$	$R\overline{3}c$	-10.41	-9.60[5]

Table S3. Constraint conditions for chemical potentials of gallium

Compounds	Constraint relation	Bounded value(eV)
GaO	$\Delta\mu_{Ga}+ \Delta\mu_{O}=\Delta H_f(GaO)$	$\Delta\mu_{Ga}$=-2.41
GaO$_2$	$\Delta\mu_{Ga}+ 2\Delta\mu_{O}=\Delta H_f(GaO_2)$	$\Delta\mu_{Ga}$=-4.52
GaO$_3$	$\Delta\mu_{Ga}+ 3\Delta\mu_{O}=\Delta H_f(GaO_3)$	$\Delta\mu_{Ga}$=-2.05
Ga$_2$O$_3$	$2\Delta\mu_{Ga}+ 3\Delta\mu_{O}=\Delta H_f(Ga_2O_3)$	$\Delta\mu_{Ga}$=-5.41
Ga$_3$O$_5$	$3\Delta\mu_{Ga}+ 5\Delta\mu_{O}=\Delta H_f(Ga_3O_5)$	$\Delta\mu_{Ga}$=-5.10
GaF$_3$	$\Delta\mu_{Ga}+ 3\Delta\mu_{F}=\Delta H_f(GaF_3)$	$\Delta\mu_{Ga}$=-10.41
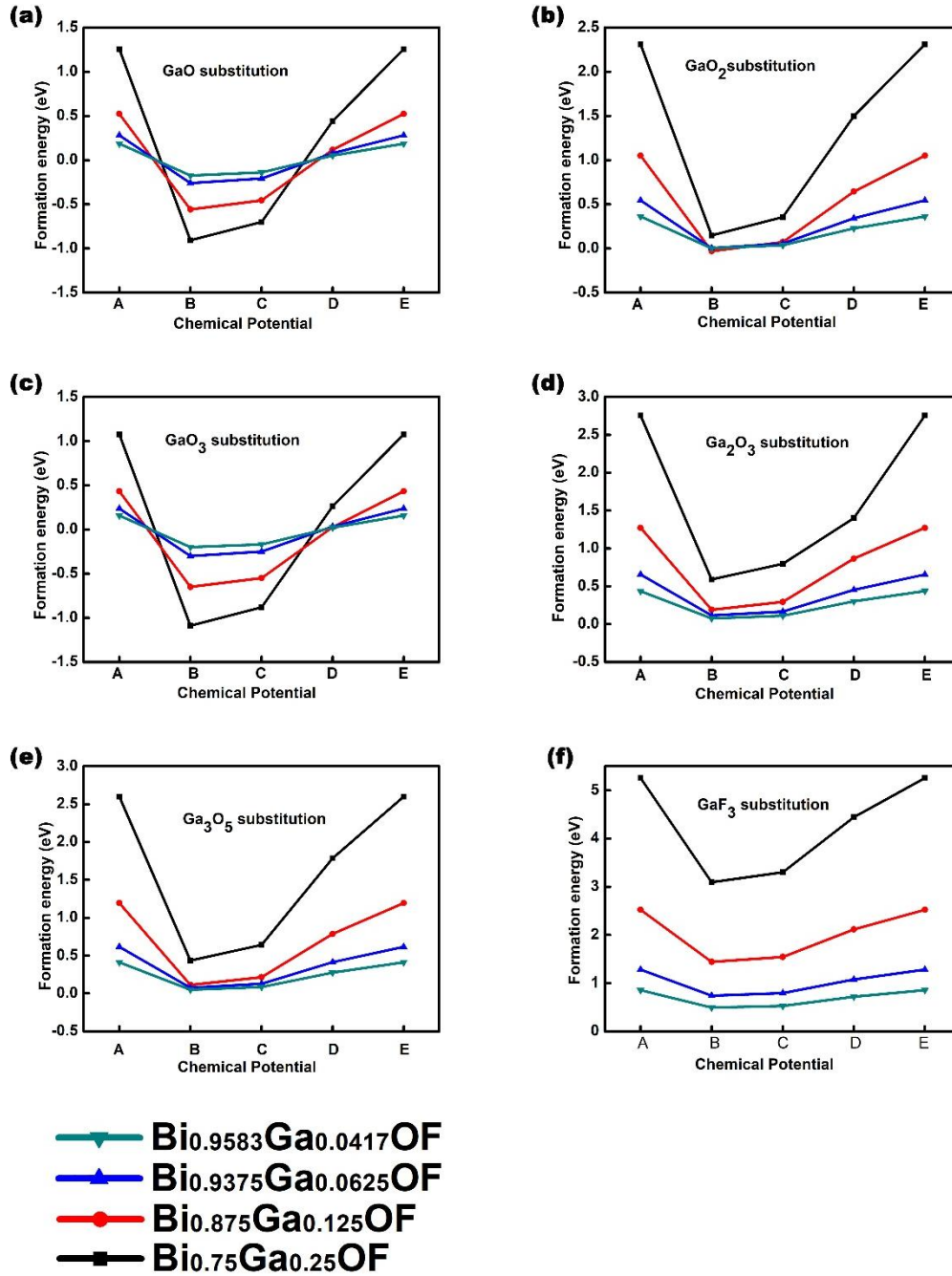
Fig. S2 The calculated formation energies of $Bi_{1-x}Ga_xOF$ ($x = 0$, 0.0417, 0.0625, 0.125, 0.25) at different chemical potentials (points A-E) via different Ga dopant. (a) GaO substitution, (b) GaO_2 substitution, (c) GaO_3 substitution, (d) Ga_2O_3 substitution, (e) Ga_3O_5 substitution and (f) GaF_3 substitution.

3. Structural properties
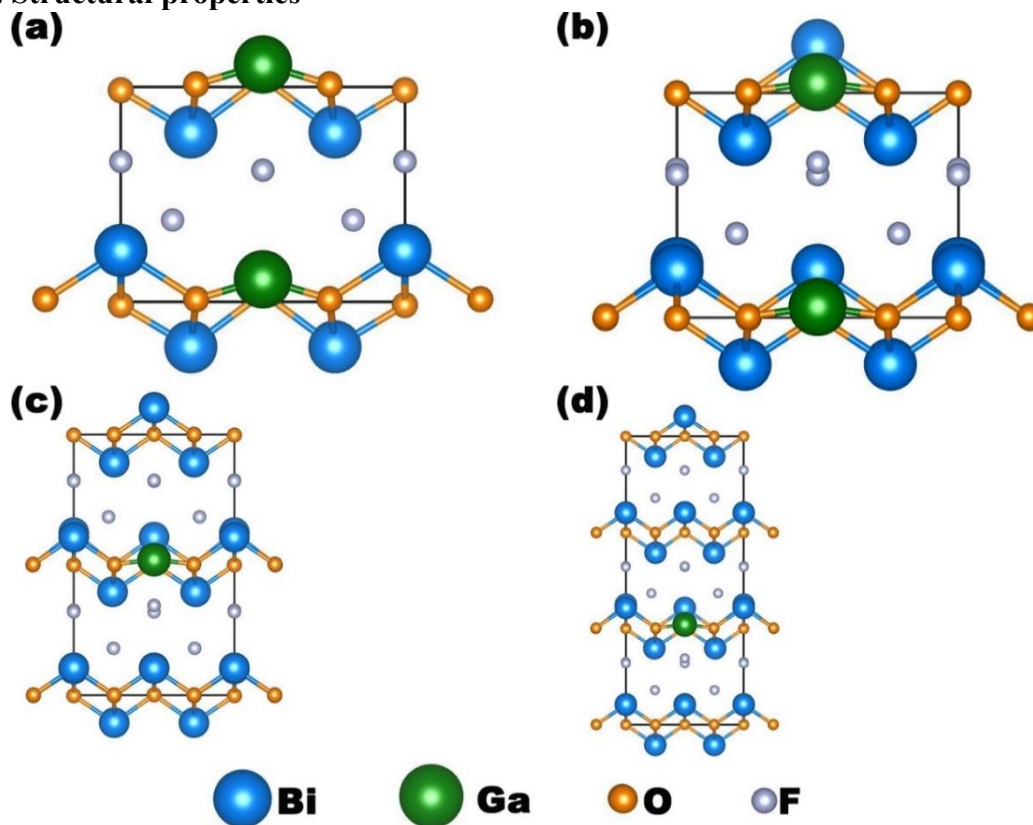
Fig.S3 The optimized structures (front view) of (a) $Bi_{0.75}Ga_{0.25}OF$, (b) $Bi_{0.875}Ga_{0.125}OF$,

(c) $Bi_{0.9375}Ga_{0.0625}OF$ and (d) $Bi_{0.9583}Ga_{0.0417}OF$.

Table S4. Lattice parameters of $Bi_{1-x}Ga_xOF$ ($x = 0$, 0.0417, 0.0625, 0.125, 0.25)

Compounds	a (Å)	b (Å)	c (Å)	α (°)	β (°)	γ (°)	V (Å³)
BiOF(Exp[6])	3.76	3.76	6.23	90	90	90	87.85
BiOF(this work)	3.79	3.79	6.23	90	90	90	89.63
$Bi_{0.9583}Ga_{0.0417}OF$	3.81	3.81	6.12	90	90	90	89.97
$Bi_{0.9375}Ga_{0.0625}OF$	3.82	3.82	6.19	90	90	90	90.09
$Bi_{0.875}Ga_{0.125}OF$	3.85	3.85	6.15	90	90	90	91.45
$Bi_{0.75}Ga_{0.25}OF$	3.89	3.83	5.88	90	90	90	88.78

For BiOF, the fluoride-ion diffusion channel(bedding void) can be roughly regarded as a rectangular cuboid(see Fig.S4(a)-(e)). Instead, for $Bi_{1-x}Ga_xOF$ (x = 0.0417, 0.0625, 0.125, 0.25), the fluoride-ion diffusion channel(bedding void) can be roughly regarded as a combination of a rectangular cuboid and a pyramid. Compared to BiOF, change rate of bedding void(ΔV_{inter}%) of $Bi_{1-x}Ga_xOF$ (x = 0, 0.0417, 0.0625, 0.125, 0.25) can be calculated. And the calculated results and detailed calculation process are given in Fig. S4 and Table S5.
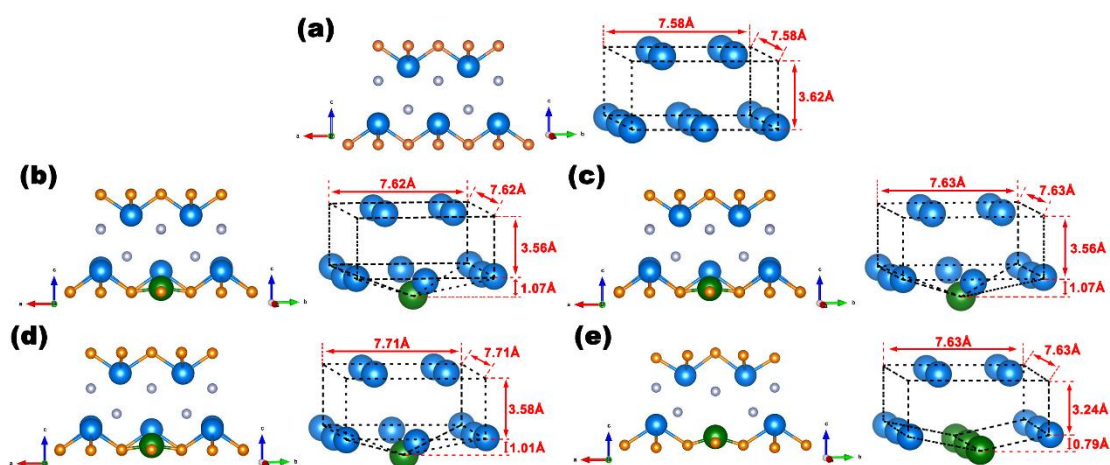
Fig. S4 Bi-Bi bedding void of (a) BiOF, (b) $Bi_{0.9583}Ga_{0.0417}OF$, (c) $Bi_{0.9375}Ga_{0.0625}OF$, (d) $Bi_{0.875}Ga_{0.125}OF$ and $Bi_{0.75}Ga_{0.25}OF$.

Table S5. The Bi-Bi bedding void rate ($\Delta V_{inter}\%$) of $Bi_{1-x}Ga_xOF$ ($x = 0$, 0.0417, 0.0625, 0.125, 0.25)

Compounds	V ($Å^3$)	change rate of bedding void($\Delta V_{inter}\%$)
BiOF	207.99	0
$Bi_{0.9583}Ga_{0.0417}OF$	227.42	9.34
$Bi_{0.9375}Ga_{0.0625}OF$	228.02	9.63
$Bi_{0.875}Ga_{0.125}OF$	232.82	11.94
$Bi_{0.75}Ga_{0.25}OF$	203.97	-1.93

4. Mechanical properties

Table S6. Elastic constants of $Bi_{1-x}Ga_xOF$ ($x = 0$, 0.0417, 0.0625, 0.125, 0.25)

x	C_{11}(GPa)	C_{12}(GPa)	C_{13}(GPa)	C_{33}(GPa)	C_{44}(GPa)	C_{66}(GPa)
0	156.07	56.17	47.34	91.71	52.71	12.73
0.0417	147.71	60.00	55.96	101.06	53.09	15.73
0.0625	152.42	64.79	62.11	82.39	52.19	18.04
0.125	144.28	62.16	60.56	101.12	42.17	14.94
0.25	127.99	60.82	47.79	83.68	46.81	16.76

After obtaining the elastic constant of $Bi_{1-x}Ga_xOF$ ($x = 0$, 0.0417, 0.0625, 0.125, 0.25), we have further calculated their Young's modulus (E), shear modulus (G), bulk modulus (B) and Poisson's ratio (v) according to formula(1)-(8)[7]. Significantly, the calculated bulk modulus(B) of BiOF is 76 GPa, which is very close to the

experimental value of 81 GPa[8]. Meanwhile, B, G, E and v of $Bi_{1-x}Ga_xOF$ ($x = 0$, 0.0417, 0.0625, 0.125, 0.25) are also given in Fig. S5.

$$B_V = \frac{2C_{11} + C_{33} + 2C_{12} + 4C_{13}}{9} \tag{1}$$

$$B_R = \frac{C^2}{C_{11} + C_{12} + 2C_{33} - 4C_{13}} \tag{2}$$

$$G_V = \frac{2C_{11} + C_{33} + 6C_{44} + 3C_{66} - C_{12} - 2C_{13}}{15} \tag{3}$$

$$G_R = \frac{15}{18(B_V / C^2) + 6/(C_{11} - C_{12}) + 6/C_{44} + 3/C_{66}} \tag{4}$$

$$C^2 = (C_{11} + C_{12})C_{33} - 2C_{13}^2 \tag{5}$$

$$B = \frac{B_V + B_R}{2}; G = \frac{G_V + G_R}{2} \tag{6}$$

$$E = \frac{9BG}{3B + G} \tag{7}$$

$$v = \frac{3B - 2G}{6B + 2G} \tag{8}$$
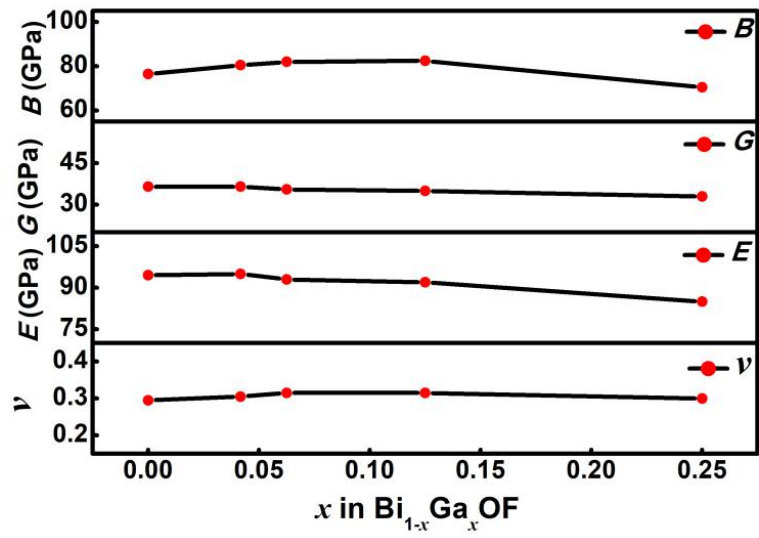
Fig. S5 B, G, E and v as a function of Ga-doping concentration (x).

5. The electronic structures of $Bi_{1-x}Ga_xOF$ (x = 0, 0.0417, 0.0625, 0.125, 0.25)
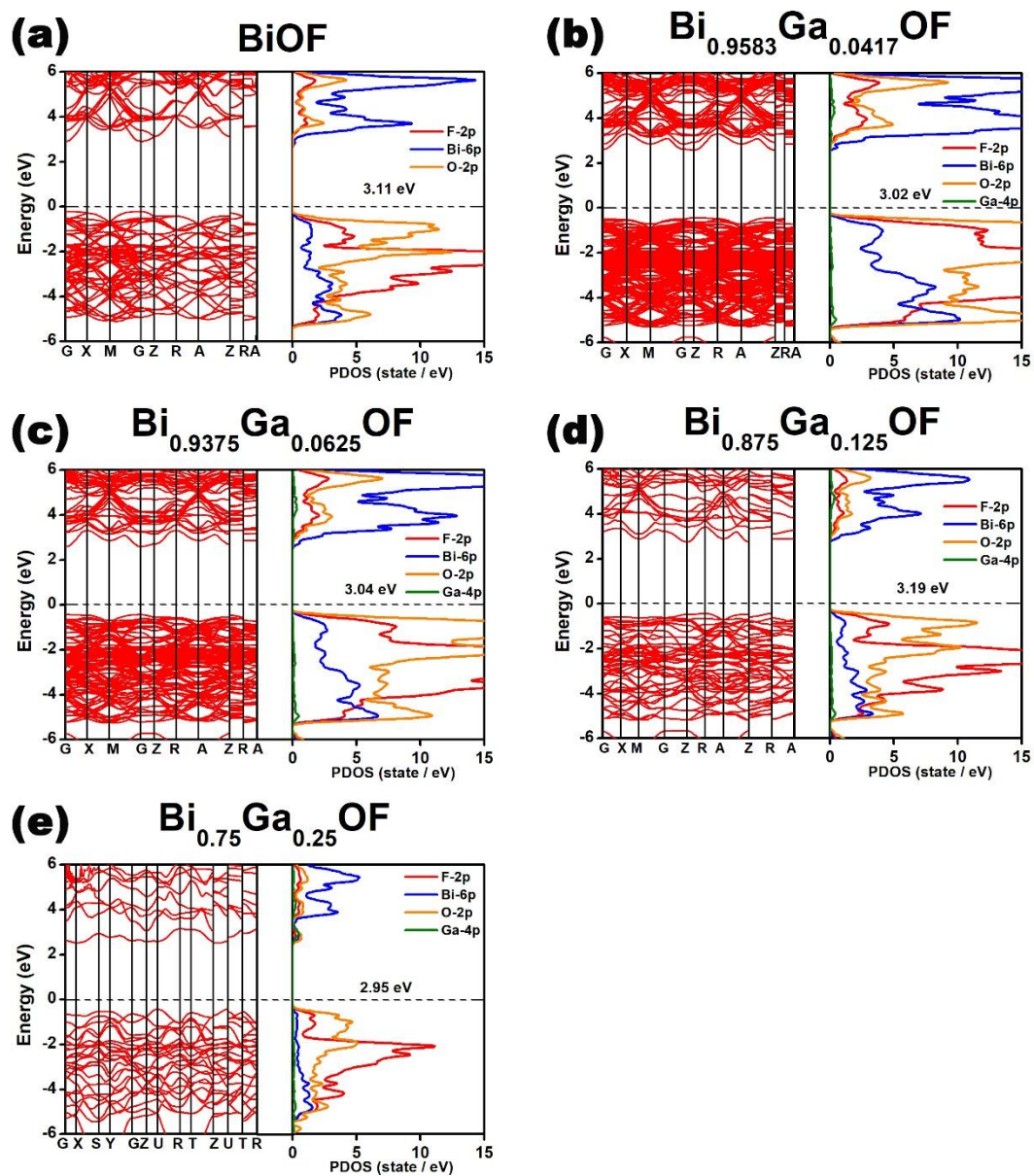
Fig. S6 Band structures and density of states (DOS) of $Bi_{1-x}Ga_xOF$ (x = 0, 0.0417, 0.0625, 0.125, 0.25).

6. AIMD results of Bi$_{1-x}$Ga$_x$OF (x = 0, 0.0417, 0.0625, 0.125, 0.25)

Here, we carried out AIMD to investigate the ionic conductivity of Bi$_{1-x}$Ga$_x$OF (x = 0, 0.0417, 0.0625, 0.125, 0.25). Firstly, we explored the diffusion behavior of fluoribe ions in BiOF. And their average mean square displacements (MSD) of F, Bi and O as a function of temperature are presented in Fig. S8. Meanwhile, the Arrhenius plot of BiOF is given in Fig. S9. According to the Arrhenius plot, we deduced that the ionic conductivity of BiOF is 7.57 × 10^{-6} S/cm at 400K, which is very close to its experimental value(3.2 × 10^{-6} S/cm at 400K[9]). Besides, we deduced that the ionic conductivity of BiOF at room temperature is 2.76 × 10^{-7} S/cm.
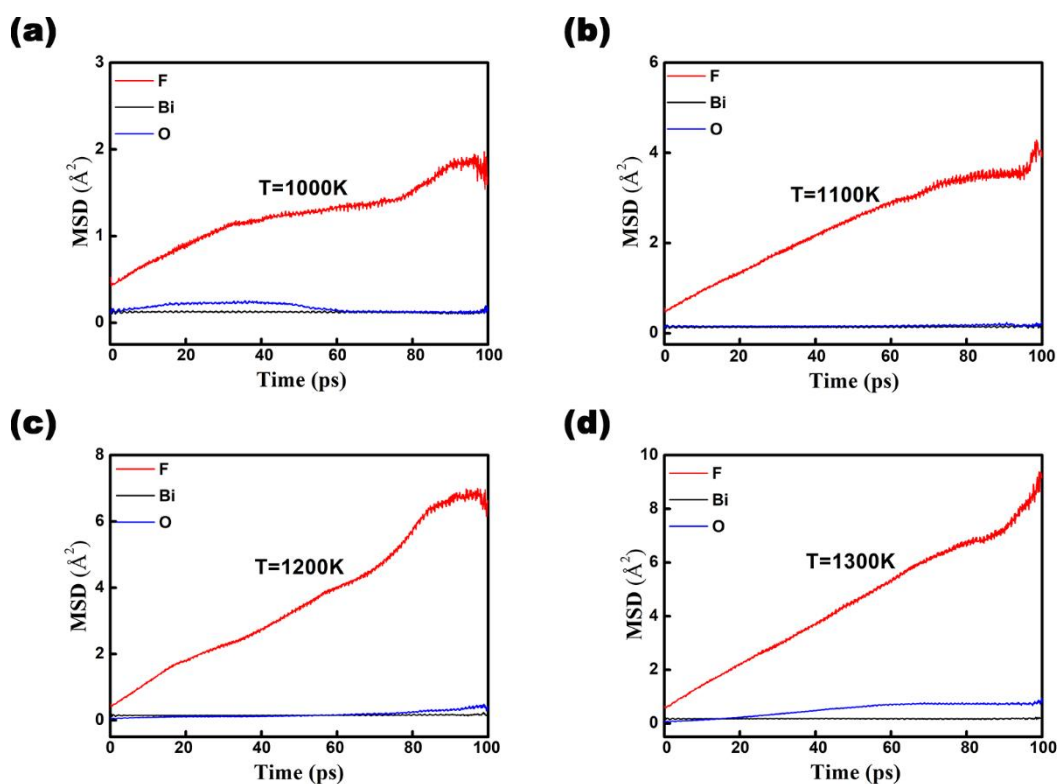
Fig. S7 Mean square displacements (MSD) for F, Bi and O ions in the BiOF at (a) 1000 K, (b) 1100 K, (c) 1200 K and (d) 1300 K.
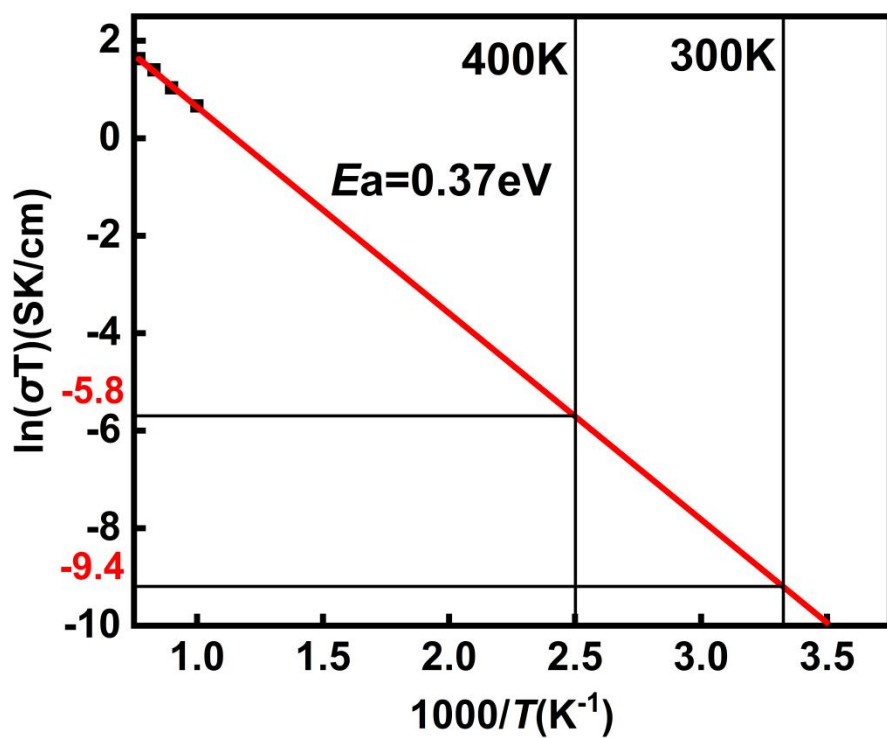
Fig. S8 Arrhenius plot of BiOF.

Similarly,AIMD results of $Bi_{1-x}Ga_xOF$ (x = 0.0417, 0.0625, 0.125, 0.25) have been obtained(see Fig. S9-Fig. S13).
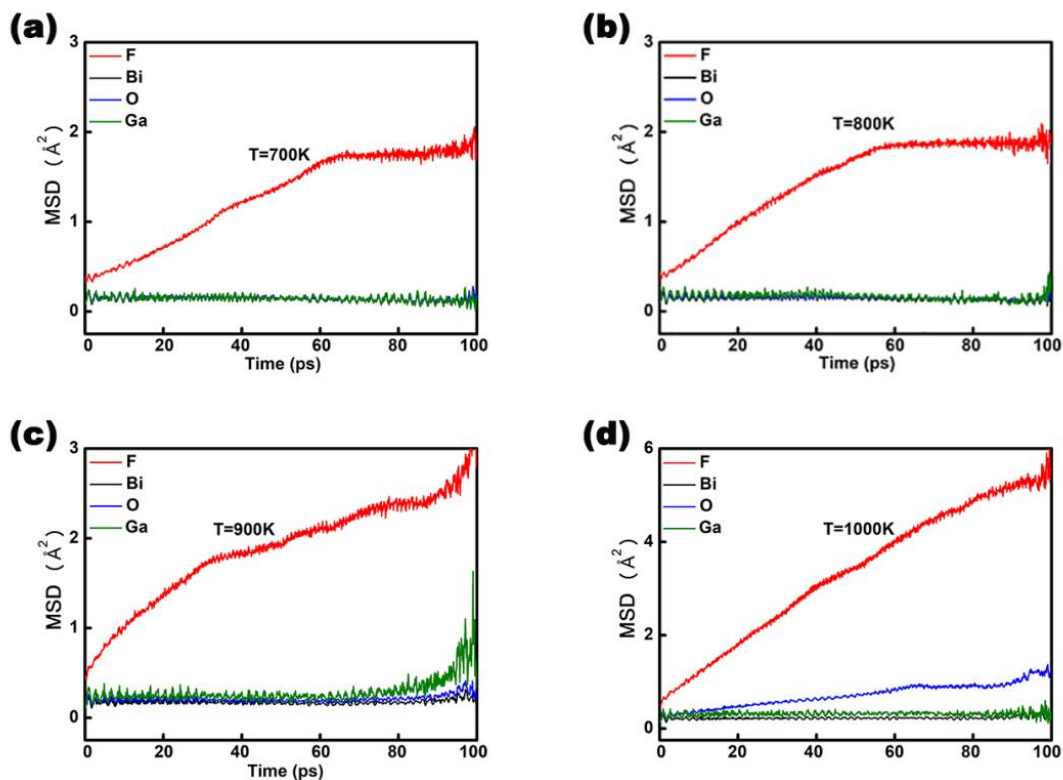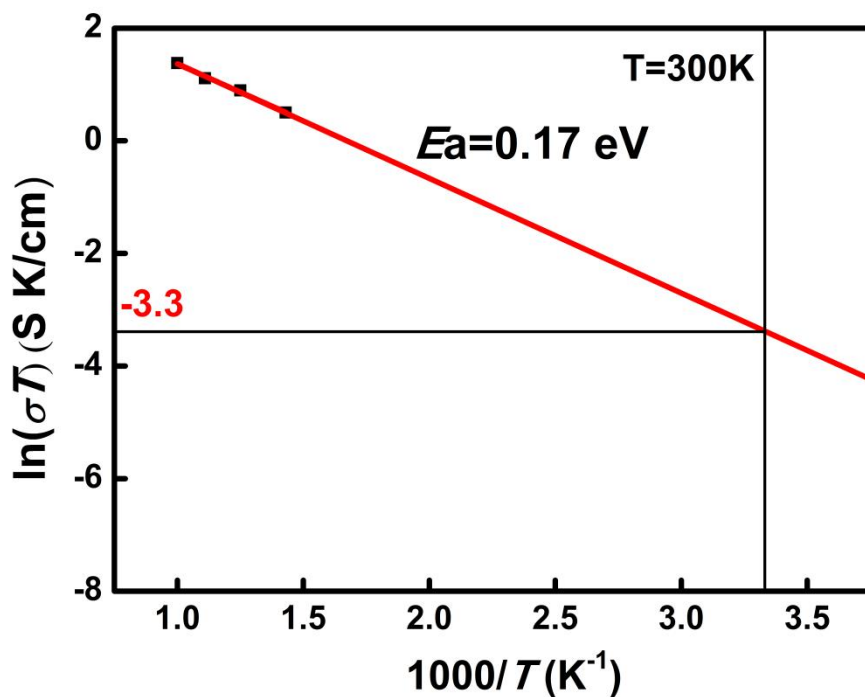
Fig.S9 Mean square displacements (MSD) for F, Bi, O and Ga ions in the $Bi_{0.9583}Ga_{0.0417}OF$ at (a) 700 K, (b) 800 K, (c) 900 K and (d) 1000 K.
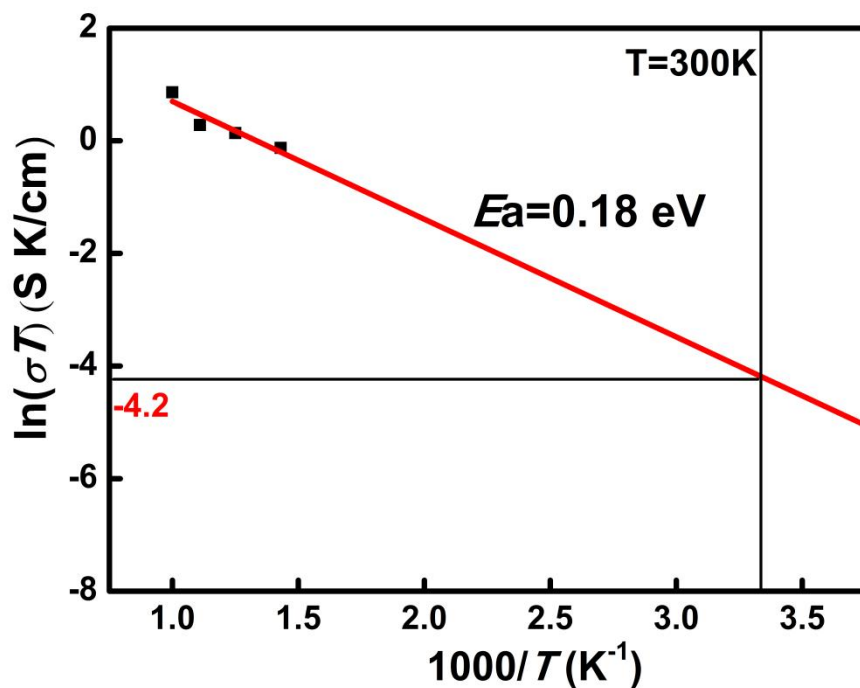
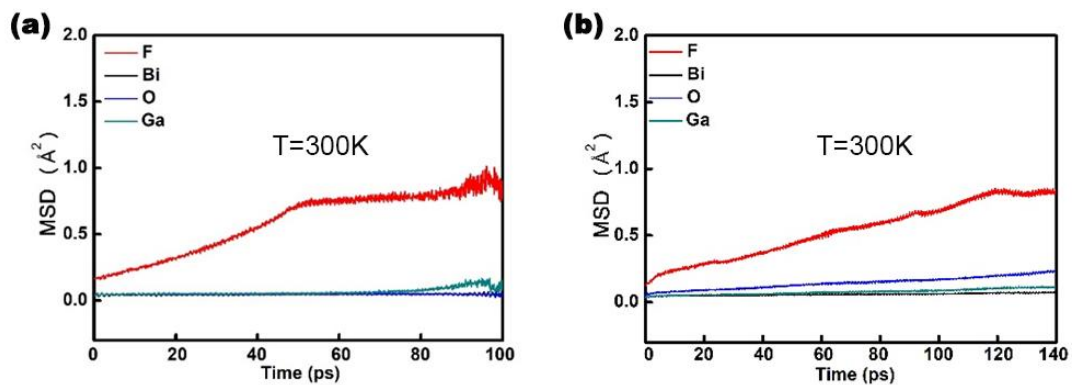**Fig. S10** Arrhenius plot of $Bi_{0.9583}Ga_{0.0417}OF$.
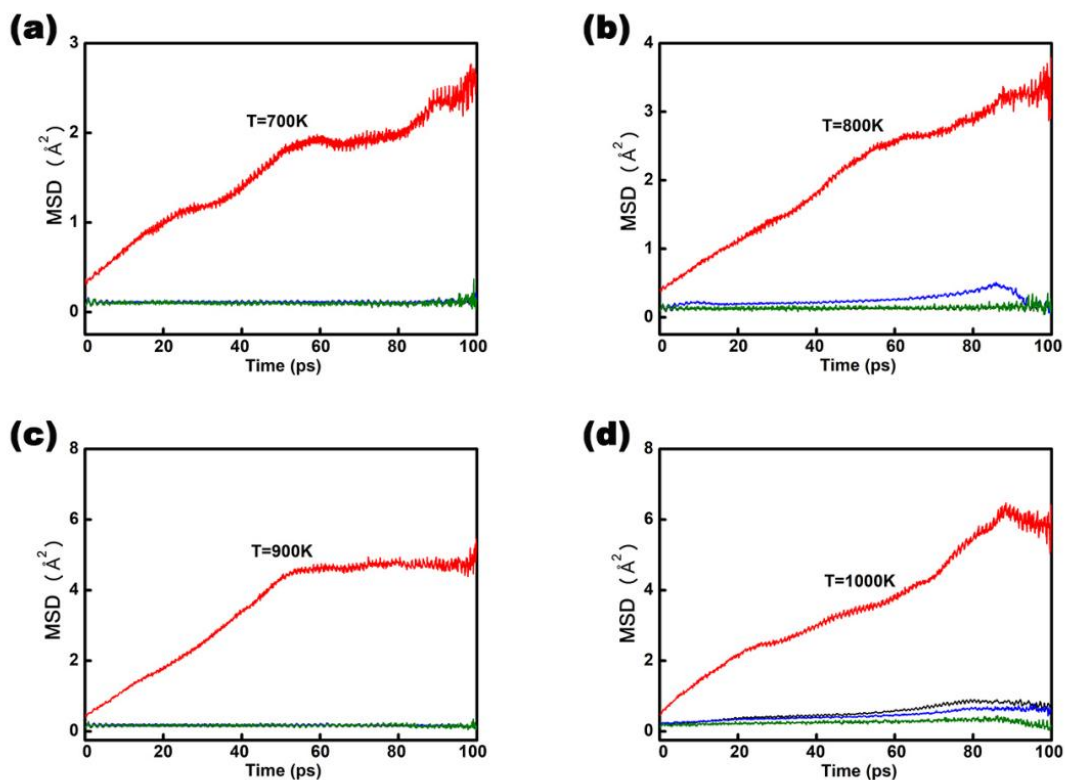
Fig. S11 Mean square displacements (MSD) for F, Bi, O and Ga ions in the Bi$_{0.9375}$Ga$_{0.0625}$OF at (a) 700 K, (b) 800 K, (c) 900 K and (d) 1000 K.

Fig. S12 Arrhenius plot of Bi$_{0.9375}$Ga$_{0.0625}$OF.

Fig. S13 Mean square displacements (MSD) for F, Bi and O ions in the (a) $Bi_{0.875}Ga_{0.125}OF$ and (b) $Bi_{0.75}Ga_{0.25}OF$.

7. Migration process of fluorine ion in the BiOF and $Bi_{0.875}Ga_{0.125}OF$
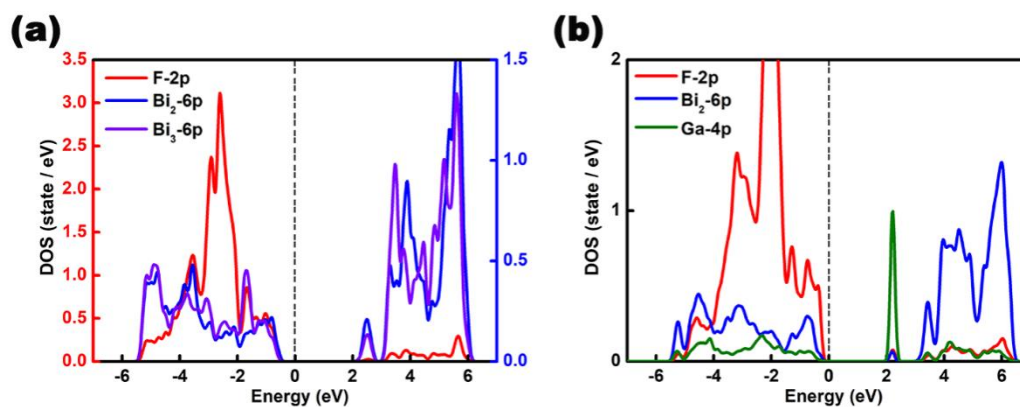
**Fig. S14** Density of states (DOS) of Bi_2-F-Bi_3 cluster and (b) Bi_2-F-Ga cluster in $Bi_{0.875}Ga_{0.125}OF$.
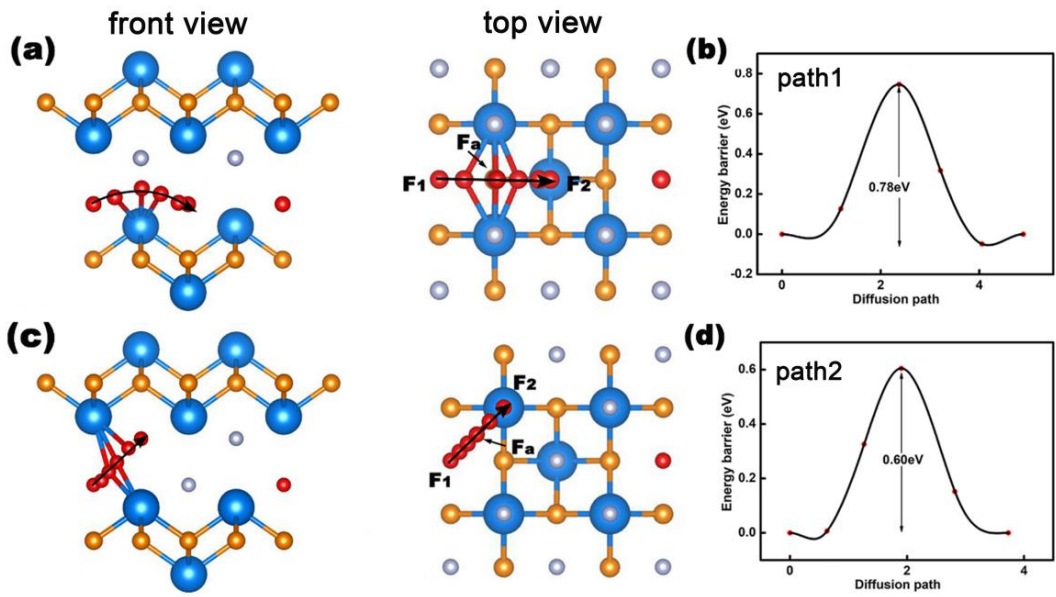
Fig. S15 (a) The front view , top view and (b) fluorine-ion diffusion energy barrier along path 1 in BiOF. (c) The front view, top view and (d) fluorine-ion diffusion energy barrier along path 2 in BiOF.
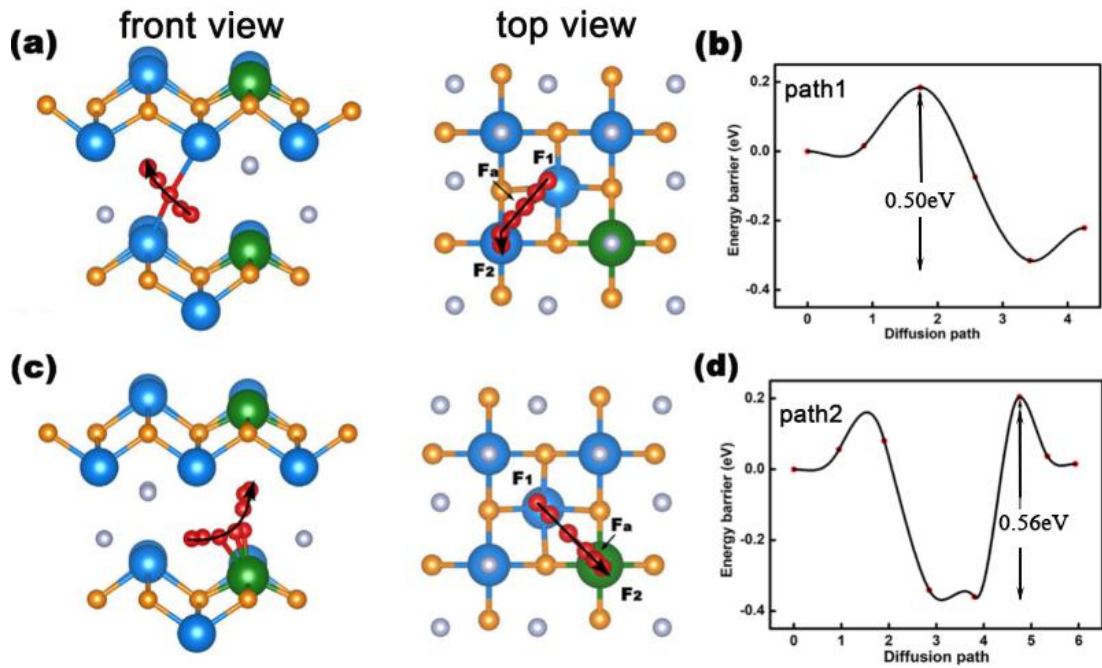
Fig. S16 (a) The front view, top view and (b) fluorine-ion diffusion energy barrier along path 1 in $Bi_{0.875}Ga_{0.125}OF$. (c) The front view, top view and (d) fluorine-ion diffusion energy barrier along path 2 in $Bi_{0.875}Ga_{0.125}OF$.
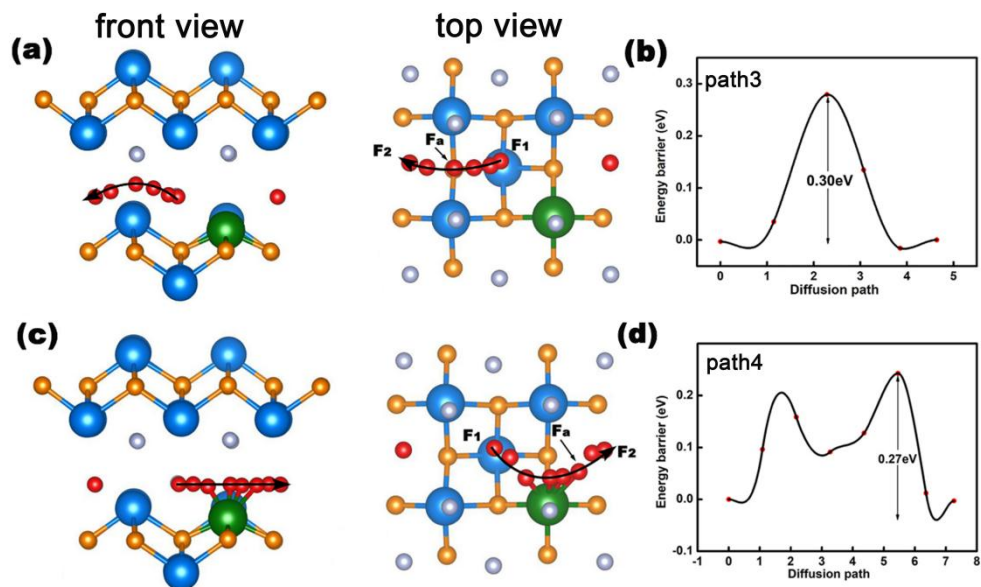
Fig. S17 (a) The front view, top view and (b) fluorine-ion diffusion energy barrier along path 3 in $Bi_{0.875}Ga_{0.125}OF$. (c) The front view, top view and (d) fluorine-ion diffusion energy barrier along path 4 in $Bi_{0.875}Ga_{0.125}OF$.
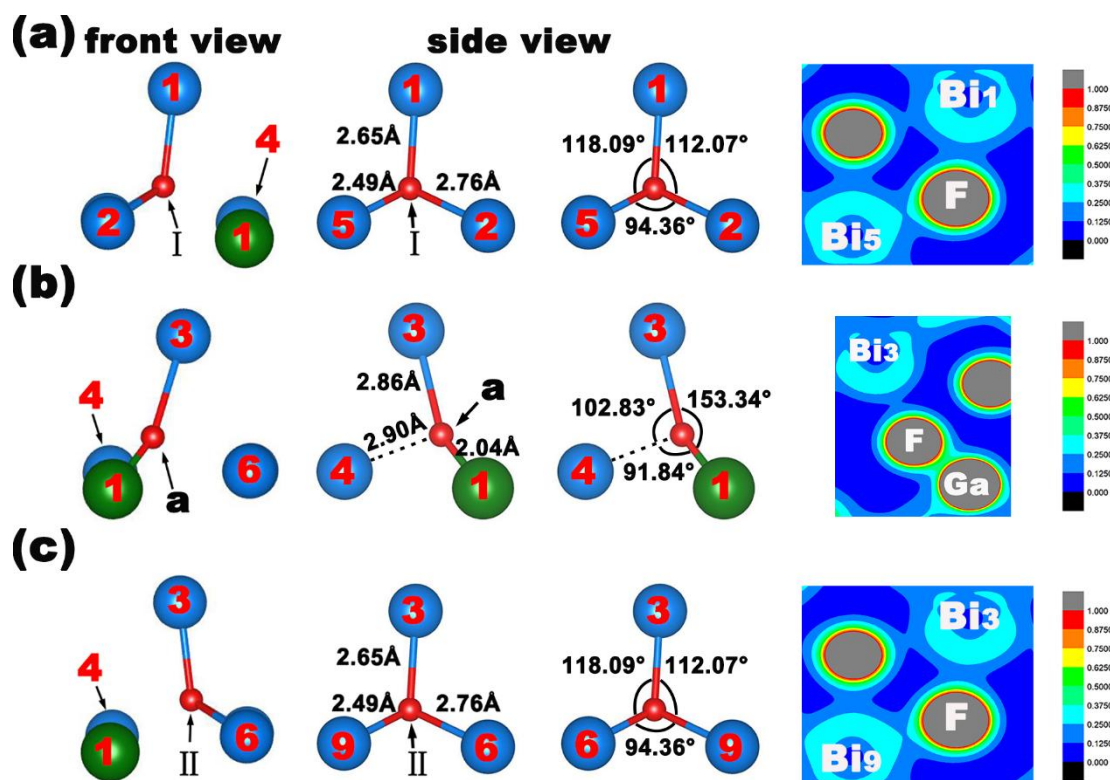
Fig. S18 Local structures and charge density at (a) initial state, (b) saddle point and (c) final state(path 4 (near the Ga dopant) in $Bi_{0.875}Ga_{0.125}OF$).
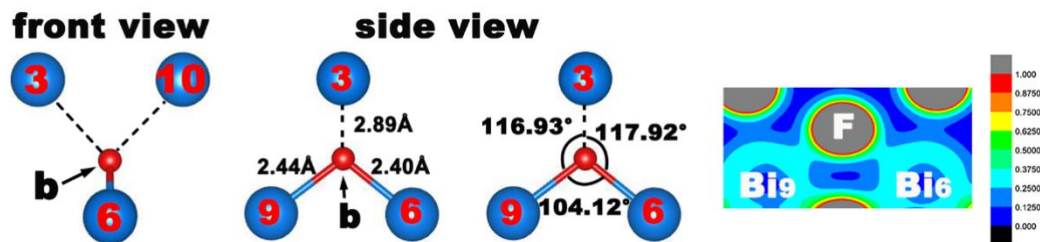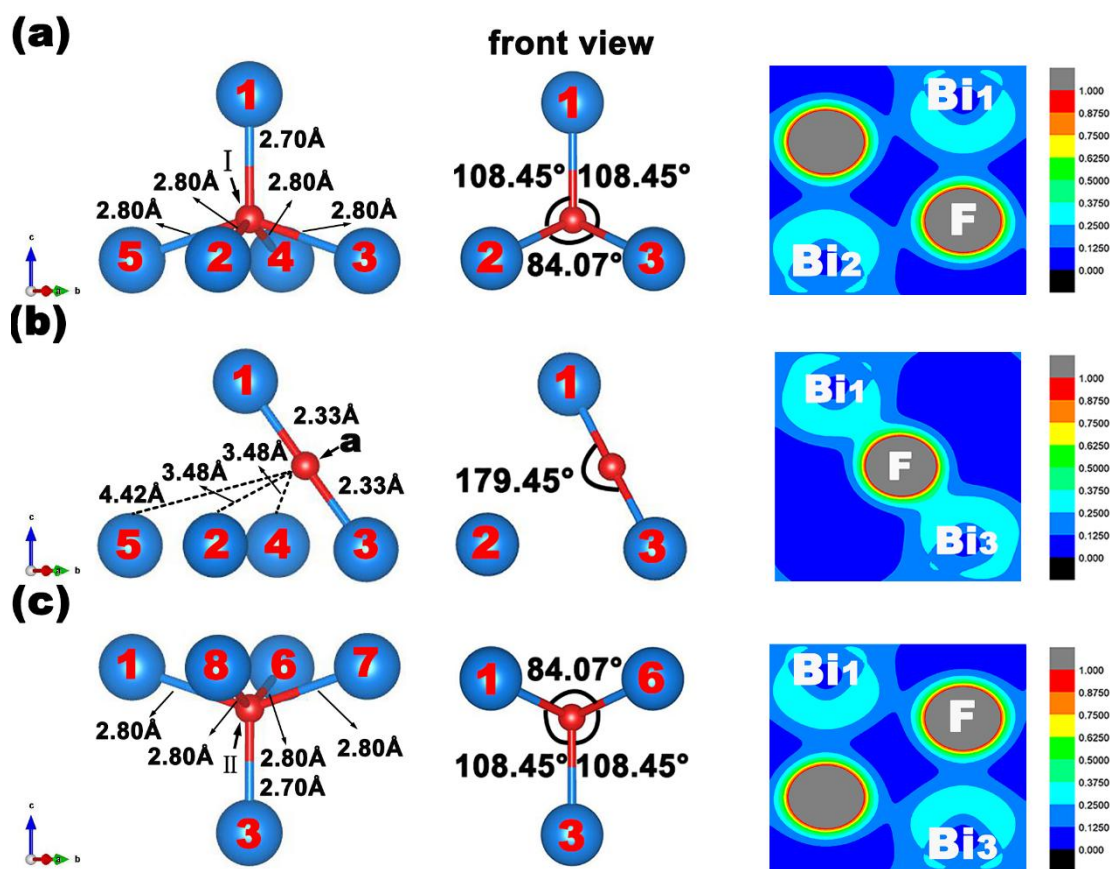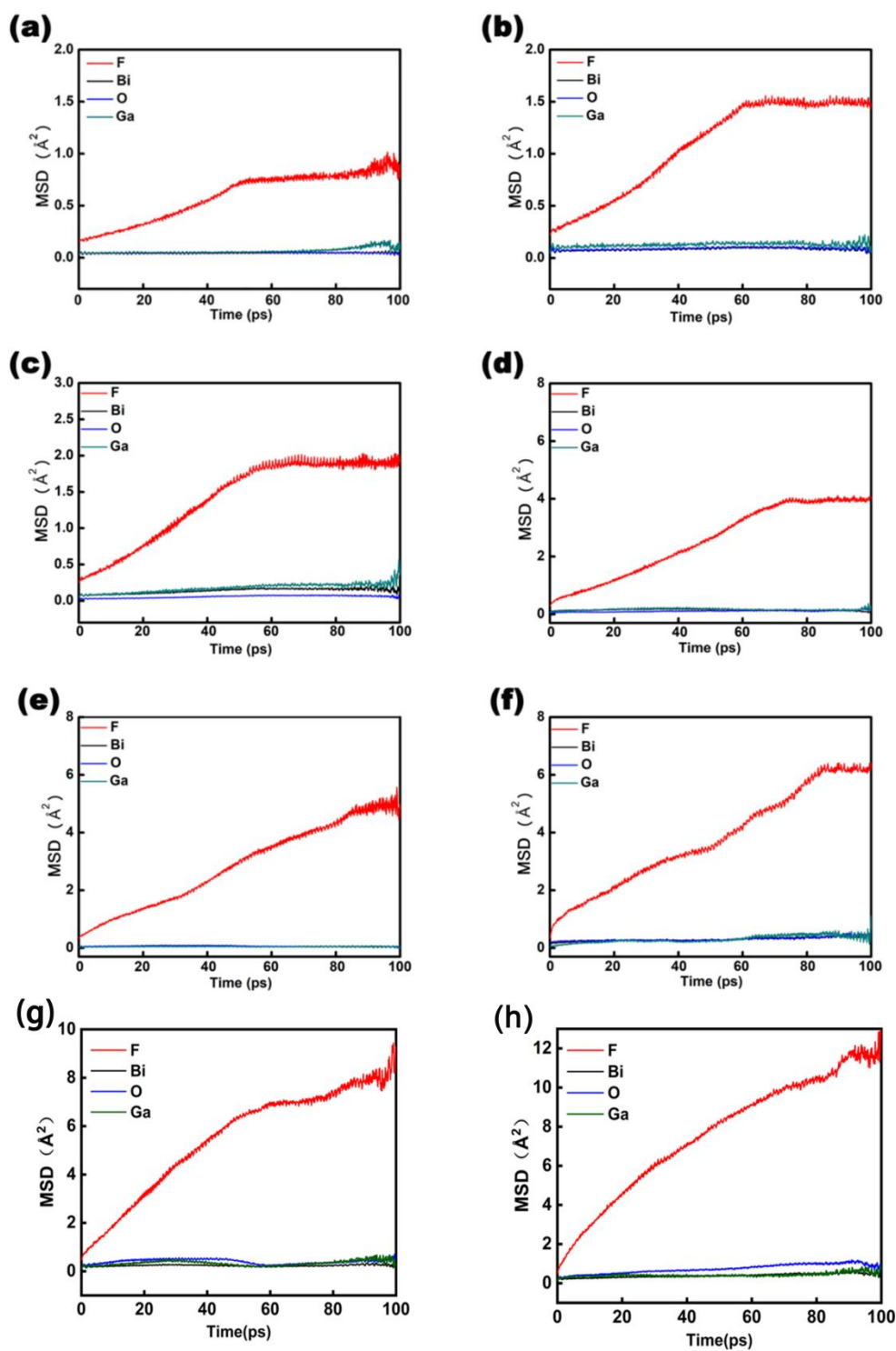
Fig. S19 Local structures and their charge density at saddle point(path 4 (far from the Ga dopant) in $Bi_{0.875}Ga_{0.125}OF$).

Fig. S20 Local structures and their charge density at (a) initial state, (b) saddle point and (c) final state(path 4 (near the Ga dopant) in BiOF).

8. The diffusion dynamics of BiOF and $Bi_{0.875}Ga_{0.125}OF$

Fig. S21 Mean square displacements (MSD) for F, Bi, O and Ga ions in $Bi_{0.875}Ga_{0.125}OF$ at (a) 300 K, (b) 400 K, (c) 500 K, (d) 600 K, (e) 700 K, (f) 800 K, (g)900K and (h)1000K
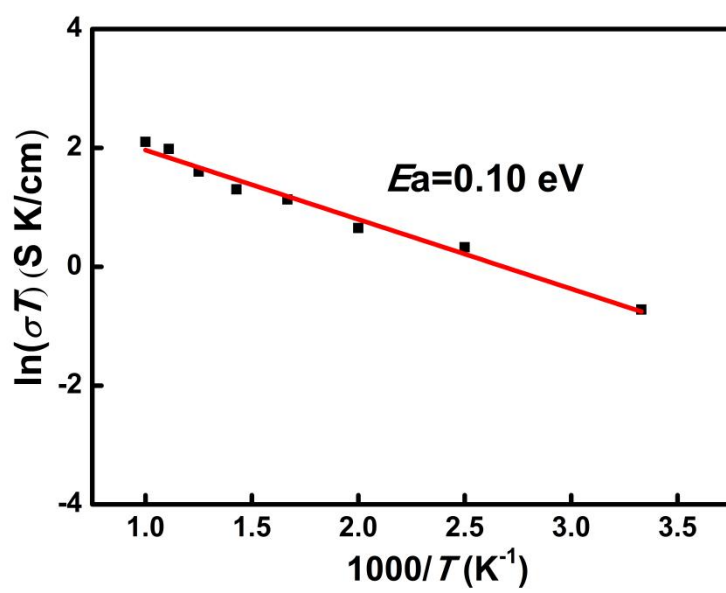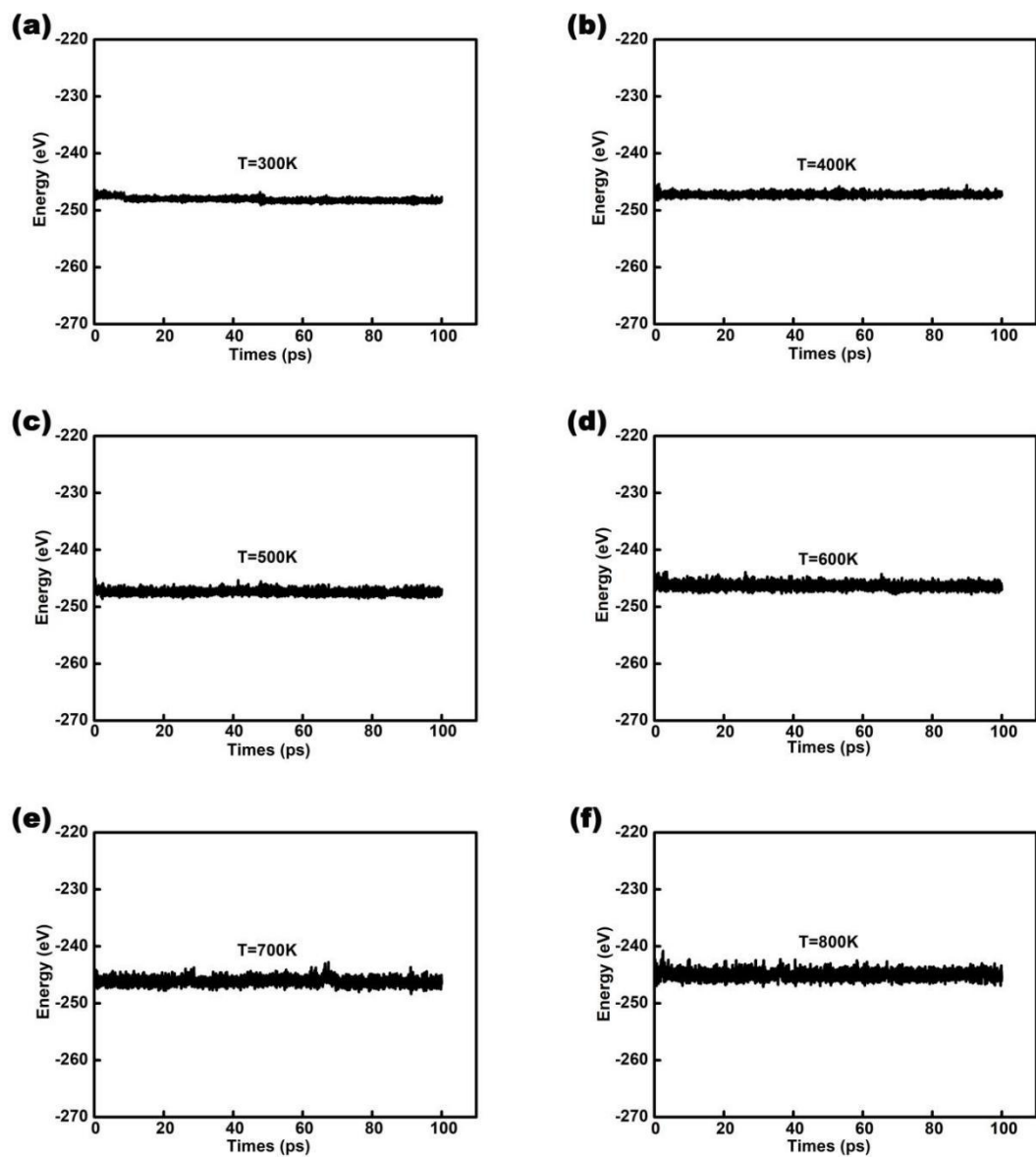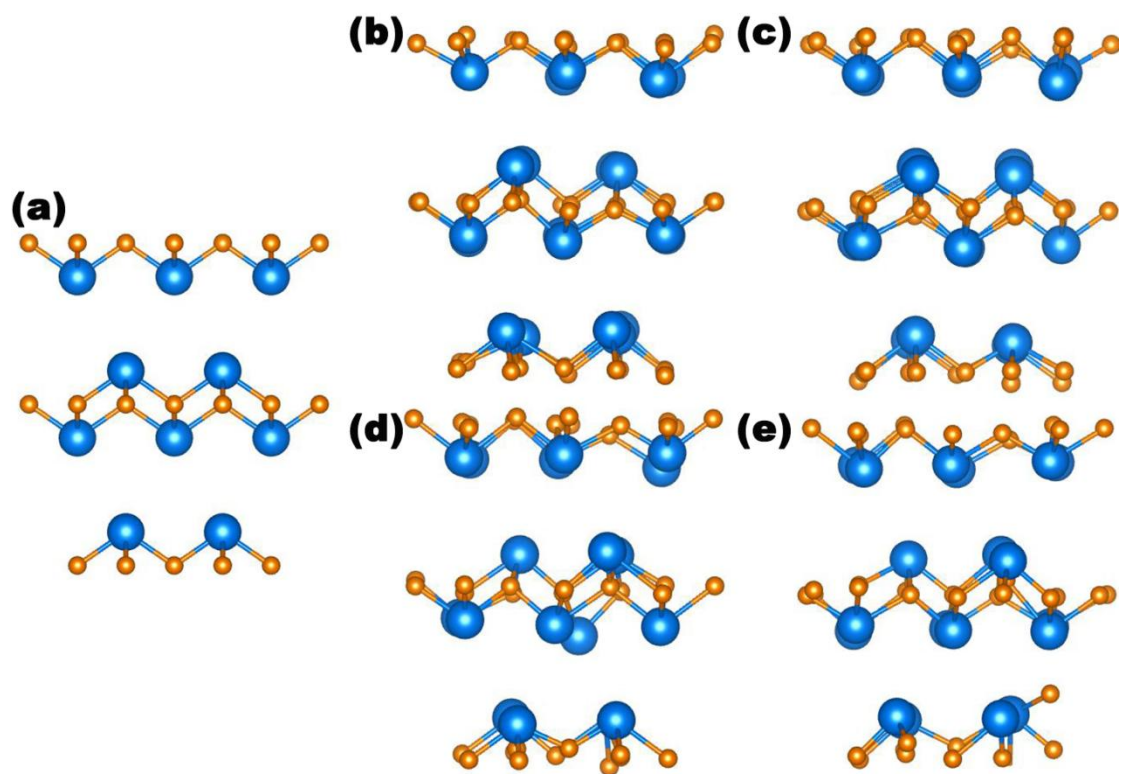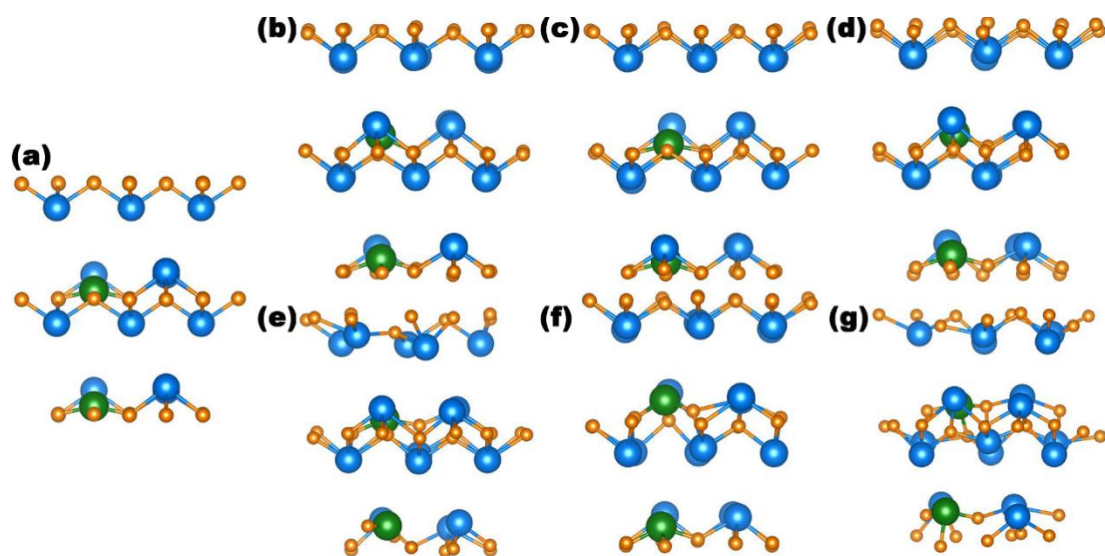
Fig. S22 Arrhenius plot of $Bi_{0.875}Ga_{0.125}OF$.

Fig. S23 Total potential energy as a function of MD time for $Bi_{0.875}Ga_{0.125}OF$ at (a) 300 K, (b) 400 K, (c) 500 K, (d) 600 K, (e) 700 K and (f) 800 K.

Fig. S24 (a) The initial and optimized structures of BiOF at (b) 1000 K, (c) 1100 K, (d) 1200 K and (e) 1300 K.

Fig. S25 (a) The initial and optimized structures of $Bi_{0.875}Ga_{0.125}OF$ at (b) 300 K, (c) 400 K, (d) 500 K, (e) 600 K, (f) 700 K and (g) 800 K.

9. Analysis of dynamical stability of $Bi_{1-x}Ga_xOF$ (x = 0, 0.0417, 0.0625, 0.125, 0.25)

In order to analyze the dynamical stability of $Bi_{1-x}Ga_xOF$ (x = 0, 0.0417, 0.0625, 0.125, 0.25), we investigated the redox reaction of Bi and O ions with Ga doping. Firstly, we calculated the Bader charge of Bi and O ions in the $Bi_{1-x}Ga_xOF$ (see Fig. S26(a)). Obviously, the Bader charges of Bi and O ions keep the stabilizing value with increasing Ga concentration (x), which indicates that Ga doping has little impact on redox reaction of Bi and O ions. Then, we plotted the density of states of BiOF and $Bi_{0.875}Ga_{0.125}OF$ (see Fig. S26(b)), it is easy to find that the hybridization between Bi-6p and O-2p orbitals show no obvious change. To sum up, BiOF and $Bi_{0.875}Ga_{0.125}OF$ have excellent dynamic stability.
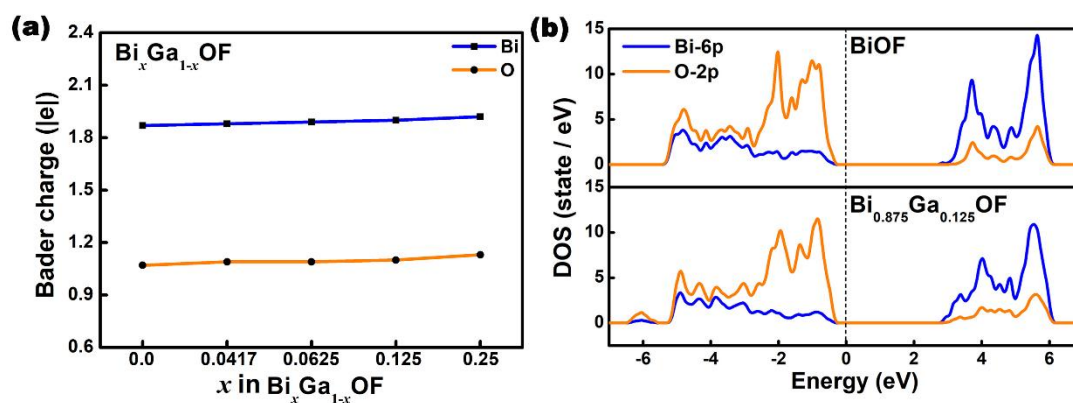
Fig. S26 (a) Bader charge of Bi and O ions in $Bi_{1-x}Ga_xOF$ (x = 0, 0.0417, 0.0625, 0.125, 0.25). (b) Density of states (DOS) of Bi and O in BiOF and $Bi_{0.875}Ga_{0.125}OF$.

10. Electrochemical stability of BiOF and $Bi_{0.875}Ga_{0.125}OF$

Table S7. Decomposition reaction for one formula unit BiOF ($Bi_8O_8F_8$)

Voltage(V)	Reaction
0	$8BiOF \rightarrow 8BiOF$
4.18	$8BiOF \rightarrow 0.7275Bi_7O_5F_{11}+2.317BiO_2+0.7275Bi$
4.41	$8BiOF \rightarrow 0.7275Bi_7O_5F_{11}+2.317O_2+2.909Bi$
4.54	$8BiOF \rightarrow 4O_2+2.6665BiF_3+5.335Bi$
8.63	$8BiOF \rightarrow 1.6BiF_5+4O_2+6.4Bi$
9.01	$8BiOF \rightarrow 4OF_2+2O_2+8Bi$

Table S8. Decomposition reaction for one formula unit $Bi_{0.875}Ga_{0.125}OF$ ($Bi_7Ga_1O_8F_8$) when Bi is acted as electrode material

Voltage(V)	Reaction
0	$Bi_7GaO_8F_8 \rightarrow 0.25Bi_7O_5F_{11}+5.25BiOF+0.5Ga_2O_3$
4.18	$Bi_7GaO_8F_8 \rightarrow 1.432BiO_2+0.7273Bi_7O_5F_{11}+0.5Ga_2O_3+0.4773Bi$
4.41	$Bi_7GaO_8F_8 \rightarrow 0.7273Bi_7O_5F_{11}+0.5Ga_2O_3+1.432O_2+1.909Bi$
4.54	$Bi_7GaO_8F_8 \rightarrow 2.667BiF_3+0.5Ga_2O_3+3.25O_2+4.333Bi$
5.09	$Bi_7GaO_8F_8 \rightarrow GaF_3+1.667BiF_3+4O_2+5.333Bi$
8.63	$Bi_7GaO_8F_8 \rightarrow BiF_5+GaF_3+4O_2+6Bi$
9.01	$Bi_7GaO_8F_8 \rightarrow GaF_3+2.75O_2+2.5OF_2+7Bi$

Table S9. Decomposition reaction for one formula unit $Bi_{0.875}Ga_{0.125}OF(Bi_7Ga_1O_8F_8)$ when Ga is acted as electrode material

Voltage(V)	Reaction
0	$Bi_7GaO_8F_8+7Ga\rightarrow2.667GaF_3+2.667Ga_2O_3+7Bi$
0.60	$Bi_7GaO_8F_8+4.333Ga\rightarrow2.667BiF_3+2.667Ga_2O_3+4.333Bi$
1.15	$Bi_7GaO_8F_8+1.909Ga\rightarrow0.7273Bi_7O_5F_{11}+1.455Ga_2O_3+1.909Bi$
1.34	$Bi_7GaO_8F_8\rightarrow0.25Bi_7O_5F_{11}+5.25BiOF+0.5Ga_2O_3$
5.52	$Bi_7GaO_8F_8\rightarrow1.909BiO_2+0.7273Bi_7O_5F_{11}+0.1818Ga_2O_3+0.6364Bi$
5.70	$Bi_7GaO_8F_8\rightarrow1.909BiO_2+0.7273Bi_7O_5F_{11}+0.2727O_2+Ga$
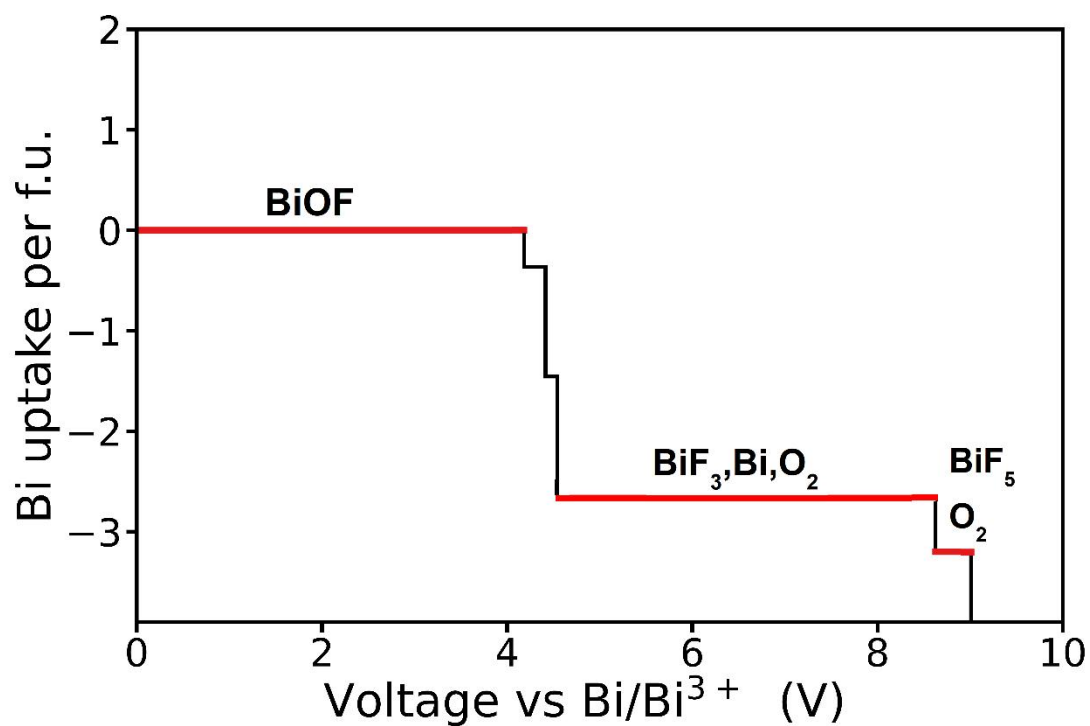
Fig. S27 Voltage profiles of BiOF.
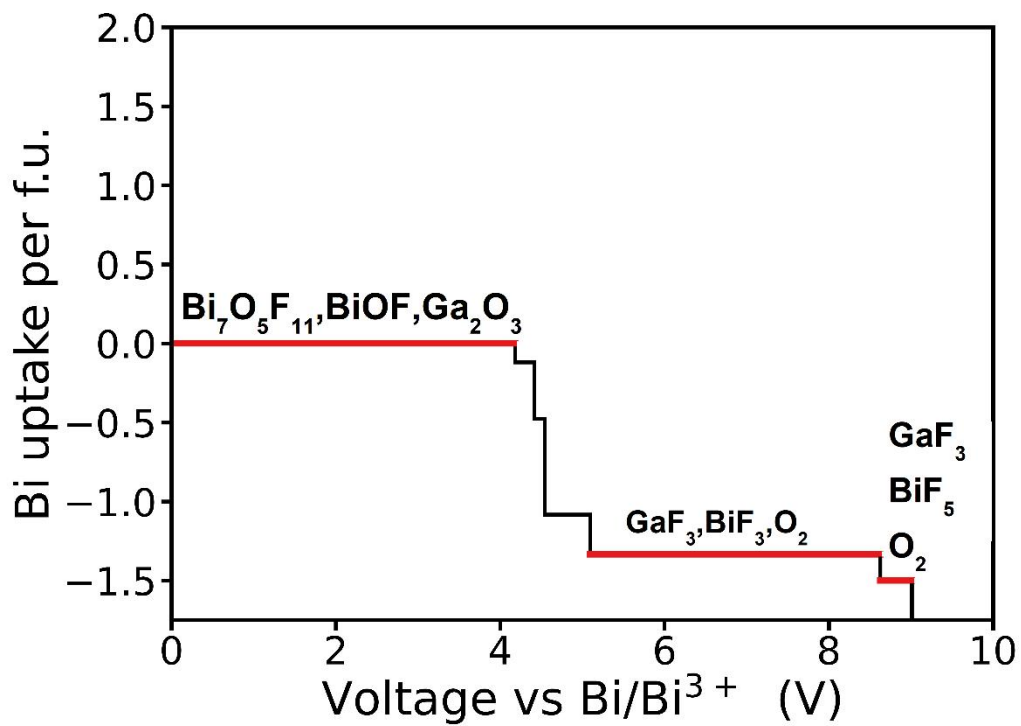
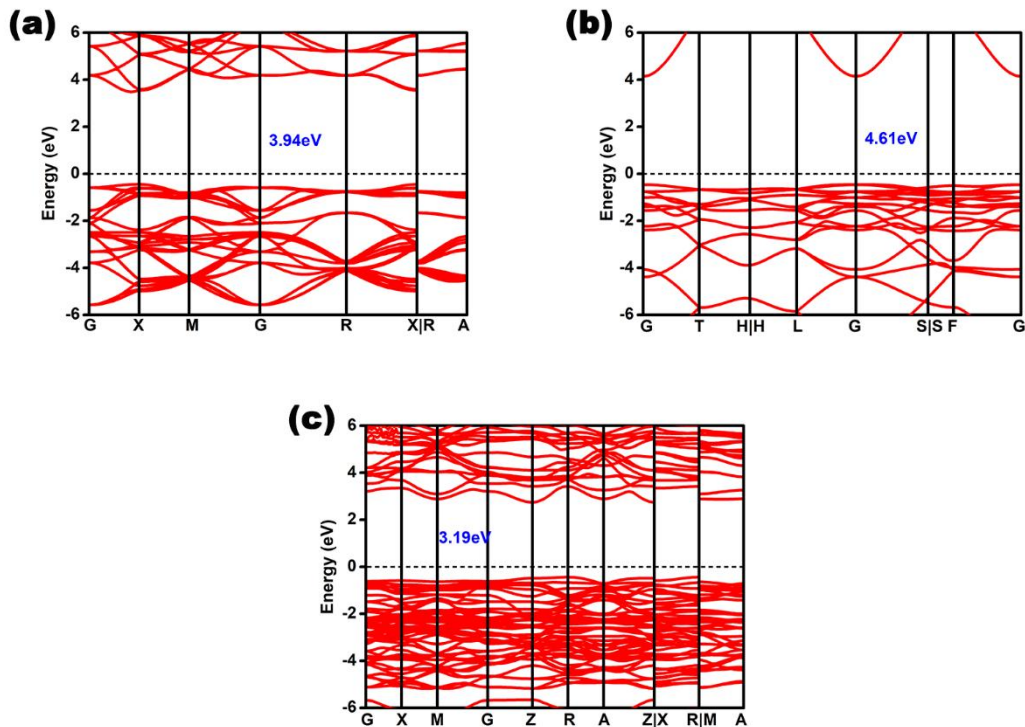**Fig. S28** Voltage profiles of $Bi_{0.875}Ga_{0.125}OF$.

Fig. S29 Band structure of (a) BiF_3, (b) GaF_3 and (c) $Bi_{0.875}Ga_{0.125}OF$.

References

1. G. Moiseev, N. Vatolin and N. Belousova, *Journal of thermal analysis and calorimetry*, 2000, **61**, 289-303.
2. Z.-X. Li, G.-Q. He, B. Kong, T.-X. Zeng and J. Zhang, *Journal of Physics and Chemistry of Solids*, 2020, **146**, 109581.
3. Z. Yang, S. Tan, Y. Huang, X. Wang and Y. Pei, *Current Applied Physics*, 2016, **16**, 12-19.
4. V. Zade, B. Mallesham, S. Shantha-Kumar, A. Bronson and C. Ramana, *Inorganic Chemistry*, 2019, **58**, 3707-3716.
5. L. Zhuravleva, M. Nikitin, I. Sorokin and L. Sidorov, *International journal of mass spectrometry and ion processes*, 1985, **65**, 253-261.
6. J. Soubeyroux, S. Matar, J. Reau and P. Hagenmuller, *Solid State Ionics*, 1984, **14**, 337-345.
7. Z.-j. Wu, E.-j. Zhao, H.-p. Xiang, X.-f. Hao, X.-j. Liu and J. Meng, *Physical Review B*, 2007, **76**, 054115.
8. S. Matar, J.-M. Reau, L. Rabardel, G. Demazeau and P. Hagenmuller, *Solid state ionics*, 1983, **11**, 77-81.
9. E. I. Ardashnikova, V. A. Prituzhalov and I. B. Kutsenok, in *Functionalized Inorganic Fluorides: Synthesis, Characterization and Properties of Nanostructured Solids*, Willey Chippenham, 2010, pp. 423-468.